Rotating skyrmion lattices by spin torques and field or temperature gradients

Karin Everschor,[1] Markus Garst,[1] Benedikt Binz,[1] Florian Jonietz,[2] Sebastian Mühlbauer,[3]
Christian Pfleiderer,[2] and Achim Rosch[1]

[1]*Institute of Theoretical Physics, University of Cologne, D-50937 Cologne, Germany*

[2]*Physik-Department E21, Technische Universität München, D-85748 Garching, Germany*

[3]*Forschungsneutronenquelle Heinz Maier Leibnitz (FRM II), Technische Universität München, D-85748 Garching, Germany*

(Received 25 April 2012; published 20 August 2012)

Chiral magnets like MnSi form lattices of skyrmions, i.e., magnetic whirls, which react sensitively to small electric currents j above a critical current density j_c. The interplay of these currents with tiny gradients of either the magnetic field or the temperature can induce a rotation of the magnetic pattern for $j > j_c$. Either a rotation by a finite angle of up to 15° or—for larger gradients—a continuous rotation with a finite angular velocity is induced. We use Landau-Lifshitz-Gilbert equations extended by extra damping terms in combination with a phenomenological treatment of pinning forces to develop a theory of the relevant rotational torques. Experimental neutron scattering data on the angular distribution of skyrmion lattices suggest that continuously rotating domains are easy to obtain in the presence of remarkably small currents and temperature gradients.

DOI: 10.1103/PhysRevB.86.054432 PACS number(s): 85.75.−d, 75.76.+j, 12.39.Dc, 75.78.−n

I. INTRODUCTION: SPIN TORQUES AND SKYRMION LATTICES

Manipulating magnetic structures by electric current is one of the main topics in the field of spintronics. By strong current pulses one can, for example, switch magnetic domains in multilayer devices,[1,2] induce microwave oscillations in nanomagnets,[3] or move ferromagnetic domain walls.[4,5] The latter effect may be used to develop new types of nonvolatile memory devices.[6] It is therefore a question of high interest to study the coupling mechanisms of currents to magnetic structures.[7,8]

Here, the recent discovery[9] of the so-called skyrmion lattice in chiral magnets like MnSi provides a new opportunity for studying the manipulation of magnetism by electric currents[10,11] both experimentally and theoretically. The skyrmions in MnSi form a lattice of magnetic whirls, similar to the superfluid whirls forming the vortex lattice in type-II superconductors. With Lorentz force transmission electron microscopy, it is possible to obtain real-space pictures of these whirls.[12,13] While in ordinary ferromagnets currents couple only to the canted spin configurations at domain walls, the peculiar magnetic structure of the skyrmion lattice allows for an efficient *bulk* coupling. Furthermore, the smooth magnetic structure of the skyrmion lattice decouples efficiently from the underlying atomic lattice and from impurities. As a consequence, it was observed[10] that the critical current density needed to affect the magnetic structure was more than five orders of magnitude smaller than in typical spin-torque experiments.

These low current densities open opportunities for new types of experiments to study quantitatively the physics of spin-transfer torques. Due to the much lower current densities it is now possible to perform spin-torque experiments in bulk materials and thus avoid the surface effects that dominate in nanoscopic samples. Moreover, for smaller currents the effects of heating and Oersted magnetic fields created by the current are suppressed.

In this paper we suggest experiments and develop a theory with the goal of exploiting the rotational motion instead of just translational motion to investigate the interplay of electric currents and moving magnetic structures. Our theory is directly motivated by recent experiments[10] where a change of orientation of the skyrmion lattice as a function of the applied electric current was observed with neutron scattering. In Ref. 10 we have shown that the rotation arises from the interplay of a tiny thermal gradient parallel to the current and the Magnus forces arising from the spin-torque coupling of current and skyrmion lattice. For example, the rotation angle could be reversed by reversing either the current direction or the direction of the thermal gradient.

The basic idea underlying the theoretical analysis of our paper is sketched in Fig. 1. In the presence of an electric current several forces act on the skyrmion lattice. First, dissipative forces try to drag the skyrmion lattice parallel to the (spin) current. Second, the interplay of dissipationless spin currents circulating around each skyrmion and the spin currents induced by the electric current lead to a Magnus force oriented perpendicular to the current for a static skyrmion lattice (for the realistic case of moving skyrmions the situation is more complicated). In the presence of any gradient across the system (e.g., a temperature or field gradient), indicated by the color gradient, these forces will vary in strength across a skyrmion domain.

As in the experiment, we assume that the gradients are tiny: on the length scale set by the skyrmion distance the gradients have negligible effects. However, on multiplying the tiny gradient with a large length, i.e., the size of a domain of the skyrmion lattice (which can be[14] several hundred micrometers), one obtains a sizable variation of the forces across the domain. These inhomogeneous forces can give rise to rotational torques. Whether the torque arises from the Magnus forces or the dissipative forces depends, however, on the relative orientation of current and gradient and also on the direction in which the skyrmion lattice drifts. Figure 1 gives a simple example: if, for example, current and gradient are parallel to each other (right panel) the forces perpendicular to the current direction (red horizontal arrows) give rise to rotational torques while the parallel forces do not contribute.

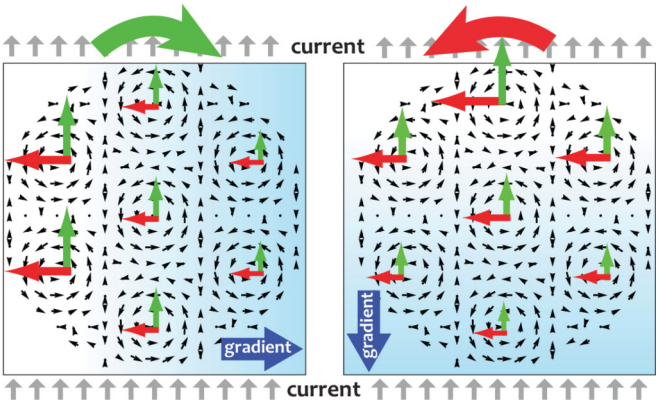

FIG. 1. (Color online) Schematic plot of the forces on a skyrmion lattice perpendicular and parallel to the current flowing in the vertical direction. For a static, nonmoving skyrmion lattice the red horizontal arrows correspond to the Magnus force and the green vertical arrows to dissipative forces. In the presence of a temperature or field gradient, these forces change smoothly across a domain, thereby inducing rotational torques which depend sensitively on the relative orientation of current and gradient (and on the direction in which the skyrmion lattice moves). Small black arrows show the local orientation of the magnetization projected into the plane perpendicular to the magnetic field $\boldsymbol{B}$. In each unit cell the magnetization winds once around the unit sphere.

The situation is reversed when current and gradient are perpendicular (left panel).

We therefore suggest using the rotation of magnetic structures as a function of the relative orientation of current and further gradients as a tool to explore the coupling of magnetism and currents. We will show that the resulting rotations depend very sensitively both on the relative size of the various forces affecting the skyrmion dynamics and on how these forces depend on the induced gradients. While we apply our theory here to skyrmion lattices, our theoretical approaches can also be used for other complex magnetic textures and our results should also have ramifications for other setups.[15,16] Quantitatively, we will only study the role of gradients induced by changes in temperature or magnetic field but other options are also possible. For example, macroscopic variations of the cross section of a sample will lead to gradients in the current density. Also changes in the chemical composition or strain in the sample can induce gradients.

It is also essential to investigate the effect of pinning of the magnetic structure by inhomogeneities arising from crystalline imperfections. Inhomogeneities distort the perfect skyrmion lattice and lead to forces prohibiting (up to a very small creep) the motion of the magnetic structure as long as the current is below a critical value, $j < j_c$. Also, for $j \gtrsim j_c$, inhomogeneities induce an effective, velocity-dependent frictional force on the moving skyrmion lattice connected to local, time-dependent distortions of the skyrmion lattice. Pinning has been widely studied both experimentally and theoretically for charge-density waves and vortex lattices in superconductors.[17–20] As the dynamics of skyrmions differs qualitatively (and quantitatively) from these two cases it is not clear which of these results can be transferred to skyrmion lattices. Due to the nonlinear dependence of the pinning forces on the velocity, they cannot be described by a simple damping term. Within this paper we will not try to develop a theory of pinning but will instead use a simple phenomenological ansatz to describe and discuss pinning effects.

Rotational torques can also arise in the absence of the types of gradients discussed above. In Ref. 21 we have studied the role of distortions of the skyrmion lattice by the underlying atomic lattice, extending the methods used by Thiele[22] to rotational torques (this method will also be used below). Such distortions indeed induce small rotational torques in a macroscopically homogeneous system, i.e., without any external gradients. Similarly, also distortions induced by disorder can induce rotational torques without external gradients, as has been discussed in the seminal paper by Schmid and Hauger.[17] But all these effects are very small and they were *not* observed in the experimental setup of Ref. 10 as no rotation was observed in the absence of gradients. Therefore they will be neglected in the following.

In the following we will first describe briefly the relevant Ginzburg-Landau model and the Landau-Lifshitz-Gilbert equation used to model the dynamics of the skyrmions. Here we include a novel damping term α' recently introduced in Refs. 23–25 (we also add the corresponding β' term). We then derive effective equations for the translational and rotational modes where pinning physics is taken into account by an extra phenomenological term. This allows us to develop predictions for both static rotations by a finite angle and continuous rotations. In the light of our results we interpret experimental results on the angular distribution of skyrmion lattices in the presence of currents and gradients.

II. SETUP

A. Ginzburg-Landau model

The starting point of our analysis is the standard Ginzburg-Landau model of a chiral magnet in the presence of a Dzyaloshinskii-Moriya interaction.[26,27] After a rescaling of the length $\boldsymbol{r}$, the local magnetization $\boldsymbol{M}(\boldsymbol{r})$, and the magnetic field $\boldsymbol{B}$ the free-energy functional reduces to[9]

$$F = \gamma_F \int d^3r \,[(1+t)\boldsymbol{M}^2 + (\nabla \boldsymbol{M})^2 + 2\,\boldsymbol{M}\cdot(\nabla \times \boldsymbol{M}) + \boldsymbol{M}^4 - \boldsymbol{B}\cdot\boldsymbol{M}]. \quad (1)$$

Here $t \propto T - T_c^{\mathrm{MF}}$ parametrizes the distance to the mean-field phase transition at $B = 0$ from a phase with helical magnetic order ($t < 0$) to a paramagnetic phase ($t > 0$).[26,27] In the presence of weak disorder t (and strictly speaking also the prefactors of all other terms) fluctuates slightly as a function of $\boldsymbol{r}$.

The skyrmion lattice (stabilized by thermal fluctuations) exists for a small temperature and field range.[9] It is translationally invariant parallel to $\boldsymbol{B}$ and shows a characteristic winding of the magnetization in the plane perpendicular to $\boldsymbol{B}$; see Fig. 1.

B. Landau-Lifshitz-Gilbert equation

To describe the dynamics of the orientation $\hat{\boldsymbol{\Omega}}(\boldsymbol{r},t) = \boldsymbol{M}(\boldsymbol{r},t)/|\boldsymbol{M}(\boldsymbol{r},t)|$ of the magnetization $\boldsymbol{M}(\boldsymbol{r},t)$ in the presence of spin-transfer torques due to electric currents, we use the

standard Landau-Lifshitz-Gilbert equation,[7,8,28,29] extended by a new dissipative term,[23–25]

$$(\partial_t + \boldsymbol{v}_s\nabla)\,\hat{\boldsymbol{\Omega}} = -\hat{\boldsymbol{\Omega}}\times\boldsymbol{H}_{\rm eff} + \alpha\,\hat{\boldsymbol{\Omega}}\times\left(\partial_t + \frac{\beta}{\alpha}\boldsymbol{v}_s\nabla\right)\hat{\boldsymbol{\Omega}} - \alpha'\left\{\hat{\boldsymbol{\Omega}}\cdot\left[\partial_i\hat{\boldsymbol{\Omega}}\times\left(\partial_t + \frac{\beta'}{\alpha'}\boldsymbol{v}_s\nabla\right)\hat{\boldsymbol{\Omega}}\right]\right\}\partial_i\hat{\boldsymbol{\Omega}}. \tag{2}$$

Here $\boldsymbol{v}_s$ is an effective spin velocity parallel to the spin-current density. More precisely, for smooth magnetic structures with constant amplitude of the magnetization, it is given by the ratio of the spin current[30] and the size of the local magnetization $|\boldsymbol{M}|$. In a good metal (for example, MnSi) $\boldsymbol{v}_s$ is expected to be parallel to the applied electric current and to depend only weakly on temperature and field. The magnetization precesses in the effective magnetic field $\boldsymbol{H}_{\rm eff} \approx -\frac{1}{M}\frac{\delta F}{\delta\hat{\boldsymbol{\Omega}}}$. Strictly speaking Eq. (2) is valid only for a constant amplitude of the magnetization, $|\boldsymbol{M}| = \text{const}$. Since $|\boldsymbol{M}|$ varies only weakly[9] in the skyrmion phase, we use as a further approximation $\boldsymbol{H}_{\rm eff} \approx -\frac{1}{M}\frac{\delta F}{\delta \boldsymbol{M}}\frac{\partial \boldsymbol{M}}{\partial\hat{\boldsymbol{\Omega}}}$ where M is the average local magnetization, $M^2 = \langle \boldsymbol{M}^2\rangle$.

The last two terms in Eq. (2) describe dissipation. α is called the Gilbert damping and β parametrizes the dissipative spin-transfer torque. The new damping term proportional to α' was introduced (for $\beta' = 0$) in Refs. 23–25. It arises from the Ohmic damping of electrons coupled by Berry phases to the spin texture as can be seen by rewriting Eq. (2) in the form

$$-\frac{\delta F}{\delta\hat{\boldsymbol{\Omega}}} = M\hat{\boldsymbol{\Omega}}\times(\partial_t + \boldsymbol{v}_s\nabla)\,\hat{\boldsymbol{\Omega}} + \alpha M\left(\partial_t + \frac{\beta}{\alpha}\boldsymbol{v}_s\nabla\right)\hat{\boldsymbol{\Omega}} + M\hat{\boldsymbol{\Omega}}\times\alpha'\left[E_i^e + \frac{\beta'}{\alpha'}(\boldsymbol{v}_s\times\boldsymbol{B}^e)_i\right]\partial_i\hat{\boldsymbol{\Omega}}, \tag{3}$$

where $E_i^e = \hat{\boldsymbol{\Omega}}\cdot(\partial_i\hat{\boldsymbol{\Omega}}\times\partial_t\hat{\boldsymbol{\Omega}})$ can be interpreted as the emergent electric field and $B_i^e = \frac{1}{2}\epsilon_{ijk}\hat{\boldsymbol{\Omega}}\cdot(\partial_j\hat{\boldsymbol{\Omega}}\times\partial_k\hat{\boldsymbol{\Omega}})$ as the emergent magnetic field.[11,31] These fields describe the forces on the electrons arising from Berry phases which they pick up when their spin adiabatically follows $\hat{\boldsymbol{\Omega}}(\boldsymbol{r},t)$. They couple to the spin rather than to the charge: electrons with magnetic moment parallel (antiparallel) to $\hat{\boldsymbol{\Omega}}$ carry the "emergent charge" $-1/2$ $(+1/2)$, respectively.[11] For $\boldsymbol{v}_s = \boldsymbol{0}$ the change of the free-energy density is given by

$$\partial_t F = \frac{\delta F}{\delta\hat{\boldsymbol{\Omega}}}\,\partial_t\hat{\boldsymbol{\Omega}} = -\alpha M(\partial_t\hat{\boldsymbol{\Omega}})^2 - \alpha' M(\boldsymbol{E}^e)^2, \tag{4}$$

which shows that the last term describes the dissipated power $\propto(\boldsymbol{E}^e)^2$ arising from the emergent electric field. $\alpha' M$ is therefore approximately given by the spin conductivity σ_s.

We have also added a new β' term. The presence of such a term becomes evident if one considers the special case of a Galilean-invariant system. In this case, all forces have to cancel when the magnetic structure is comoving with the conduction electrons, $\hat{\boldsymbol{\Omega}}(\boldsymbol{r},t) = \hat{\boldsymbol{\Omega}}(\boldsymbol{r} - \boldsymbol{v}_s t)$. This is possible only for $\alpha = \beta$ and $\alpha' = \beta'$. Solids are not Galilean invariant and therefore β' is different from α' but one can, nevertheless, expect that the two quantities are of similar order of magnitude.

Which of the damping terms will dominate? As pointed out in Refs. 23–25, the naive argument, that the α' terms are suppressed compared to the α terms as they contain two more derivatives, is not correct. The distance apart of skyrmions is[9] proportional to $1/\lambda_{\rm SO}$, where $\lambda_{\rm SO}$ parametrizes the strength of spin-orbit coupling. While the α' term has two more gradients compared to the α term, the contribution arising from α' is, nevertheless, of the same order in powers of $\lambda_{\rm SO}$, if we assume that α arises only from spin-orbit coupling, $\alpha \propto \lambda_{\rm SO}^2$, while $\alpha' \propto \lambda_{\rm SO}^0$ [Ohmic damping (see above) does not require spin-orbit effects]. As furthermore α is proportional to a scattering rate while α' is proportional to a conductivity and therefore the scattering time,[23–25] α' and β' might be the dominating damping terms in good metals.

III. DYNAMICS OF SKYRMIONS

Our goal is to describe both the drift and the rotation of the skyrmion lattice in the limit of small current densities and small magnetic or thermal gradients. We therefore assume that $\boldsymbol{v}_s$ is small compared to all characteristic velocity scales of the skyrmion lattice [e.g., $k_B(T_c - T)/\hbar$ multiplied by the skyrmion distance]. The gradients should be so small that the total change across a domain of radius r_d remains small, $r_d\nabla\lambda \ll \lambda$, where λ is B or $T_c - T$ for magnetic or thermal gradients, respectively. In this limit, both the drift velocities $v_d \lesssim v_s$ and the angular velocity $\partial_t\phi \propto \boldsymbol{v}_s\cdot\nabla\lambda$ characterizing rotational motion remain small. Below we will show that even $\partial_t\phi\, r_d$, the velocity at the boundary of the domain, remains small in the considered limit.

We can therefore neglect macroscopic deformations of the magnetic structure and consider the following ansatz:

$$\hat{\boldsymbol{\Omega}}(\boldsymbol{r},t) = \boldsymbol{R}_{\phi(t)}\cdot\hat{\boldsymbol{\Omega}}_0\big(\boldsymbol{R}_{\phi(t)}^{-1}\cdot(\boldsymbol{r} - \boldsymbol{v}_d t)\big). \tag{5}$$

Here $\hat{\boldsymbol{\Omega}}_0(\boldsymbol{r})$ describes the static skyrmion lattice, $\boldsymbol{R}_\phi$ is a matrix describing a rotation by the angle ϕ around the direction of the skyrmion lines (i.e., around the field direction when anisotropies are neglected, which will be assumed in the following), and $\boldsymbol{v}_d t$ describes the location of the center of the skyrmion domain. This ansatz describes a magnetic domain which rotates around its center, while the center is moving with the velocity $\boldsymbol{v}_d$. When the torque forces are too weak to induce a steady-state rotation, such that $\partial_t\phi = 0$, we will study rotations by the finite angle ϕ as in the experiment of Ref. 9. The ansatz (5) neglects the interface dynamics and interactions between different domains. We will argue below that the corresponding forces and torques can be neglected in the limit of large domains. More importantly, we will have to take into account pinning forces which arise from local distortions of the skyrmion lattice at impurities; see below. This effect is not included in Eq. (5) which assumes a rigid lattice.

A. Drift of domains

To obtain an equation for the drift velocity $\boldsymbol{v}_d$ we follow Thiele[22] and project Eq. (3) onto the translational mode by multiplying Eq. (3) with $\partial_i\hat{\boldsymbol{\Omega}}$ and integrating over a unit cell (UC). We thereby obtain to order $(\nabla\lambda)^0$ (where no rotations occur) an equation for the force per two-dimensional (2D)

magnetic unit cell (and per length)[32]

$$\begin{aligned}
&\boldsymbol{G}\times(\boldsymbol{v}_s-\boldsymbol{v}_d)+\boldsymbol{\mathcal{D}}(\tilde{\beta}\boldsymbol{v}_s-\tilde{\alpha}\boldsymbol{v}_d)+\boldsymbol{F}_{\rm pin}=\boldsymbol{0},\\
&G_i=\int_{\rm UC} d^2r\, M B_i^e=\mathcal{G}\hat{B}_i,\quad \mathcal{G}=4\pi MW,\\
&\mathcal{D}_{ij}=\int_{\rm UC} d^2r\, M\partial_i\hat{\boldsymbol{\Omega}}\,\partial_j\hat{\boldsymbol{\Omega}}=\mathcal{D}\boldsymbol{P}_{ij},\\
&\mathcal{D}'=\int_{\rm UC} d^2r\, M\,(\boldsymbol{B}^e)^2,\\
&\tilde{\alpha}=\alpha+\alpha'\mathcal{D}'/\mathcal{D},\quad \text{and}\quad \tilde{\beta}=\beta+\beta'\mathcal{D}'/\mathcal{D},
\end{aligned}\tag{6}$$

where $\hat{\boldsymbol{B}}=\boldsymbol{B}/|\boldsymbol{B}|$. Here the first term describes the Magnus force, proportional to the topological winding number W, which is for the skyrmion lattice exactly given by $W=-1$. $\boldsymbol{G}$ is called the gyromagnetic coupling vector, following Thiele.[22] The second term represents the dissipative forces with the projector $\boldsymbol{P}$ into the plane perpendicular to $\boldsymbol{B}$, $\boldsymbol{P}=(\mathbb{1}-\hat{\boldsymbol{B}}\cdot\hat{\boldsymbol{B}}^T)$.

Besides the forces discussed above, pinning forces, described by the last term in Eq. (6), also have to be considered. Formally, they are encoded in spatial fluctuations of $\delta F/\delta\hat{\boldsymbol{\Omega}}$ in Eq. (3). The Thiele approach, used above, which considers only a global shift (or a global rotation;[21] see below) of the magnetic structure does not capture these pinning effects, as for a perfectly rigid magnetic structure, random pinning forces average to zero, such that no net effect remains in the limit of a large domain. To describe pinning, it is necessary[17,18] to take into account that the magnetic structure adjusts locally to the pinning forces, a complicated problem for which presently no full solution exists[20,33] and which is far beyond the scope of the present paper. Instead, we use a phenomenological ansatz and write for a finite drift velocity $\boldsymbol{v}_d$ with direction $\hat{\boldsymbol{v}}_d=\boldsymbol{v}_d/|\boldsymbol{v}_d|$

$$\boldsymbol{F}_{\rm pin}=-4\pi M v_{\rm pin} f(v_d/v_{\rm pin})\,\hat{\boldsymbol{v}}_d \tag{7}$$

to describe a net pinning force, which is oriented opposite to the direction of motion. Its strength, which depends both on the number (and nature) of defects responsible for pinning and on the elastic properties of the skyrmion lattice, is parametrized by the "pinning velocity" $v_{\rm pin}$. The function $f(x)$ with $f(x\to 0)=1$ and $f(x\to\infty)=x^{\nu}$ parametrizes the nonlinear dependence of the pinning force on the velocity. Presently, it is not clear to what extent $f(x)$ depends on microscopic details, and also the exponent ν is not known. For large driving velocities, however, pinning becomes less and less important ($\nu<1$).[19,20,33] If the driving forces are smaller than the force $4\pi M v_{\rm pin}$ needed to depin the lattice, v_d vanishes and the pinning forces cancel exactly the driving forces. Note that we do not consider creep, i.e., a tiny motion driven by thermal (or quantum) fluctuations, which occurs even in the pinning regime.[20] If the dissipative forces can be neglected, it is in principle possible to obtain $f(x)$ from a measurement of the velocity of the skyrmion lattice.[11]

In the limit $v_s\gg v_{\rm pin}$, where $\boldsymbol{F}_{\rm pin}$ can be neglected, we solve Eq. (6) for $\boldsymbol{v}_s\perp\boldsymbol{B}$ to obtain

$$\boldsymbol{v}_d=\frac{\tilde{\beta}}{\tilde{\alpha}}\boldsymbol{v}_s+\frac{\tilde{\alpha}-\tilde{\beta}}{\tilde{\alpha}^3(\mathcal{D}/\mathcal{G})^2+\tilde{\alpha}}\left(\boldsymbol{v}_s+\tilde{\alpha}\frac{\mathcal{D}}{\mathcal{G}}\hat{\boldsymbol{B}}\times\boldsymbol{v}_s\right). \tag{8}$$

B. Rotational torques

By symmetry, a small uniform current cannot induce any rotational torques on a skyrmion lattice with perfect sixfold rotation symmetry and therefore all effects arise from gradients. To derive an equation for the rotational torques which determine the rotations around the $\boldsymbol{B}$ axis, we follow[21,34,35] a similar procedure as used for the translations by multiplying Eq. (3) by the generator of rotations applied to $\hat{\boldsymbol{\Omega}}$,

$$\partial_\phi\hat{\boldsymbol{\Omega}}=\hat{\boldsymbol{B}}\times\hat{\boldsymbol{\Omega}}-[\hat{\boldsymbol{B}}(\Delta\boldsymbol{r}\times\boldsymbol{\nabla})]\hat{\boldsymbol{\Omega}}, \tag{9}$$

with $\Delta\boldsymbol{r}=\boldsymbol{r}-\boldsymbol{v}_d t$ and integration over $\boldsymbol{r}$. This procedure leads to several types of contribution.

For the first type of contribution, we observe that the second term in Eq. (9), linear in $\Delta\boldsymbol{r}$, is much larger than the first one, which we can therefore neglect whenever the second term contributes. The second term induces torques of the form $\boldsymbol{r}\times\boldsymbol{f}$ where the force f_i is obtained by multiplying $\nabla_i\hat{\boldsymbol{\Omega}}$ with the terms of Eq. (3). In the presence of gradients of the parameter λ we obtain

$$\begin{aligned}
\int d^2r\,\hat{\boldsymbol{B}}\cdot[\boldsymbol{r}\times\boldsymbol{f}(\lambda(\boldsymbol{r}))]&\approx\int d^2r(\hat{\boldsymbol{B}}\cdot[\boldsymbol{r}\times\partial_\lambda\boldsymbol{f}])(\boldsymbol{r}\cdot\boldsymbol{\nabla}\lambda)\\
&\approx\frac{A}{4\pi}\hat{\boldsymbol{B}}\cdot\left[\boldsymbol{\nabla}\lambda\times\partial_\lambda\int\boldsymbol{f}\right],
\end{aligned}\tag{10}$$

where A is the area of the domain. Here it is essential to take the derivative with respect to λ for *fixed* $\boldsymbol{v}_d$, reflecting that due to the rigidity of the skyrmion crystal $\boldsymbol{v}_d$ is constant across the domain. As the sum of all relevant forces vanishes [Eq. (6)], $\sum_i\boldsymbol{f}_i(\lambda,\boldsymbol{v}_d)=0$, one obtains $\frac{d}{d\lambda}\sum_i\boldsymbol{f}_i=0$ while $\frac{\partial}{\partial\lambda}\sum_i\boldsymbol{f}_i|_{\boldsymbol{v}_d}$ is finite. In Eq. (10) we have implicitly assumed a symmetrically shaped domain, where integrals odd in $\boldsymbol{r}$ vanish. In general, there will also be a shape-dependent torque $\mathcal{T}_{\rm shape}$ arising even in the absence of a gradient. As its sign is random, it can easily be distinguished from the other torques (and appears to be relatively small in the MnSi experiments).[9] More difficult is the question of what happens at the interface of different domains or when a domain comes close to the surface of the sample. Nominally, surface forces are suppressed by a factor proportional to $1/\sqrt{A}$ compared to the bulk terms considered above, but the relevant prefactors are difficult to estimate. We will neglect in the following formulas both extra surface forces and shape-dependent torques.

A different contribution arises from the time derivatives $\partial_t\hat{\boldsymbol{\Omega}}=\partial_t\phi\,\partial_\phi\hat{\boldsymbol{\Omega}}-(\boldsymbol{v}_d\boldsymbol{\nabla})\hat{\boldsymbol{\Omega}}$ in Eq. (3). The contribution proportional to $\boldsymbol{v}_d$ is of the form discussed above. The term proportional to $\partial_t\phi$ leads to extra torques independent of $\boldsymbol{\nabla}\lambda$. By combining the linear term in Δr from $\partial_\phi\hat{\boldsymbol{\Omega}}$ with the second term of Eq. (9) we obtain for example the contribution $\alpha\,\partial_t\phi\int M\{(\hat{\boldsymbol{B}}[\Delta\boldsymbol{r}\times\boldsymbol{\nabla}])\boldsymbol{\Omega}\}^2$ which is also linear in A. Physically this term describes the frictional torque which is linear in the angular velocity $\partial_t\phi$. The frictional torque per volume is proportional to A because the velocity and therefore the frictional forces grow linearly with the distance from the center of the rotating domain.

Finally, a contribution exists which is independent of the gradients $\boldsymbol{\nabla}\lambda$, of the angular velocity $\partial_t\phi$, and of $\boldsymbol{v}_s$. This contribution describes that in the absence of any external perturbation the skyrmion lattice has a preferred orientation relative to the atomic lattice. Such terms express that angular

momentum can be transferred directly from the skyrmion lattice to the underlying atomic lattice, mediated by spin-orbit coupling and small anisotropy terms [not included in Eq. (1)]. These terms have been discussed in detail in Ref. 21. This torque per unit cell,

$$\mathcal{T}_L = -\int_{\mathrm{UC}} d^2r\, \frac{\delta F}{\delta \hat{\boldsymbol{\Omega}}}(\hat{\boldsymbol{G}}_{\mathrm{rot}}\hat{\boldsymbol{\Omega}}) = -\frac{\partial F_{\mathrm{UC}}}{\partial \phi} \approx -\chi\ \sin(6\phi), \tag{11}$$

can be expressed by the change of free energy per unit cell, F_{UC}, upon rotation by the angle ϕ, where $\phi = 0$ reflects the equilibrium position and $\sin 6\phi$ reflects the sixfold symmetry of the skyrmion lattice. As has been discussed in Ref. 10, the absolute value of χ in materials like MnSi is tiny as it arises only to high order in spin-orbit coupling and, in contrast to all other terms, it is not linear in the size of the domain. Nevertheless, we have to consider this term, as it is the leading contribution arising to zeroth order in $\nabla\lambda$ and $\boldsymbol{v}_s$.

Balancing all torques (per unit cell) we obtain as our central result

$$\begin{aligned} 0 &= \mathcal{T}_L + \mathcal{T}_G + \mathcal{T}_{\mathrm{pin}} + \mathcal{T}_{\mathcal{D}}, \\ \mathcal{T}_G &= \frac{A}{4\pi}\nabla\lambda \cdot \left[\frac{\partial(\mathcal{G}\boldsymbol{v}_s)}{\partial\lambda} - \frac{\partial\mathcal{G}}{\partial\lambda}\boldsymbol{v}_d\right], \\ \mathcal{T}_{\mathrm{pin}} &= \frac{A}{4\pi}\nabla\lambda \cdot [\hat{\boldsymbol{B}} \times \hat{\boldsymbol{v}}_d]\frac{\partial F_{\mathrm{pin}}}{\partial\lambda}, \quad F_{\mathrm{pin}} \equiv |\boldsymbol{F}_{\mathrm{pin}}|, \\ \mathcal{T}_{\mathcal{D}} &= -\frac{A\tilde{\alpha}\mathcal{D}}{2\pi}\partial_t\phi \\ &\quad - \frac{A}{4\pi}\nabla\lambda \cdot \left[\hat{\boldsymbol{B}} \times \left(\frac{\partial(\mathcal{D}\tilde{\beta}\boldsymbol{v}_s)}{\partial\lambda} - \frac{\partial(\mathcal{D}\tilde{\alpha})}{\partial\lambda}\boldsymbol{v}_d\right)\right]. \end{aligned} \tag{12}$$

The dependence of the torques on the relative orientation of velocities and currents, is for $\boldsymbol{v}_d = 0$ (and $\partial_t\phi = 0$), fully consistent with the simple picture shown in Fig. 1: the dissipative torques $\mathcal{T}_D$ arise when gradient and current are perpendicular to each other while the reactive torque $\mathcal{T}_G$ arising from the Magnus force is activated for a parallel alignment of gradients and currents. For finite $\boldsymbol{v}_d$, however, this simple intuitive picture cannot be used, especially as some of the torques tend to cancel when $\boldsymbol{v}_d$ approaches $\boldsymbol{v}_s$.

C. Rotation angle and angular velocity

Equation (12) can be rewritten in the compact form

$$\sin 6\phi = -\gamma\ \partial_t\phi + \nabla\lambda \cdot \boldsymbol{V}_s, \tag{13}$$

where $\gamma = \frac{A\tilde{\alpha}\mathcal{D}}{2\pi\chi}$ and the vector $\boldsymbol{V}_s = \boldsymbol{V}_s[\boldsymbol{v}_s]$ can be obtained by first solving Eq. (6) to obtain $\boldsymbol{v}_d$ as a function of $\boldsymbol{v}_s$. This function is inserted into Eq. (12) which, finally, is devided by $-\chi$. The function $\boldsymbol{V}_s[\boldsymbol{v}_s]$ with $\boldsymbol{V}_s[0] = 0$ is proportional to the area A of the domain and encodes all information on how the current couples to small gradients and includes contributions from Magnus forces, dissipative forces, and pinning.

1. Dependence on size of gradients

Qualitatively, three different regimes have to be distinguished. For $j < j_c$, when pinning forces cancel all reactive and dissipative forces, there is neither a motion nor a rotation of the skyrmion lattice, $\boldsymbol{V}_s = \boldsymbol{0}, \phi = 0$, within our approximation. Note, however, that it is well known from the physics of charge-density waves or vortices[20] that even below j_c a slow creep motion is possible. Whether during this creep rotations are also possible is unclear, but the rather sharp onset of the rotation in the experiments of Ref. 10 (see Fig. 8) seems to contradict a scenario of pronounced rotations during creep. For $j > j_c$, the domains move and $\boldsymbol{V}_s$ will generally be finite. In this case, one can control the size and direction of rotations by the size of $\nabla\lambda$ as shown in Fig. 2. For $|\nabla\lambda \cdot \boldsymbol{V}_s| < 1$, one obtains a solution where $\partial_t\phi = 0$ but the gradients induce a rotation by a finite angle

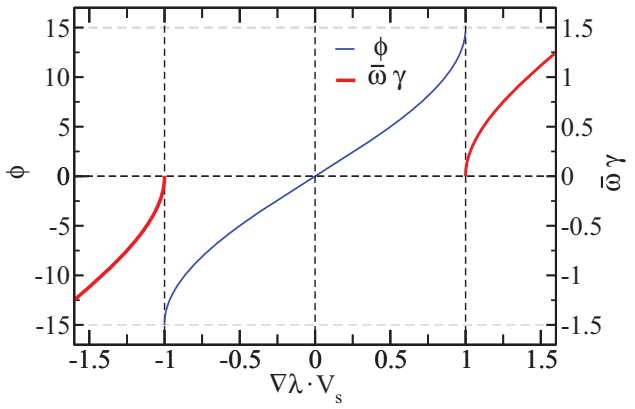

FIG. 2. (Color online) Rotation angle ϕ (in units of 1°) and angular velocity $\bar{\omega}$ (times the prefactor γ) as a function of $\nabla\lambda \cdot \boldsymbol{V}_s$ determined from Eq. (13).

$$\phi = \tfrac{1}{6}\arcsin \nabla\lambda \cdot \boldsymbol{V}_s, \tag{14}$$

which grows upon increasing $\nabla\lambda$ from zero until it reaches the maximal possible value $\pi/12 = 15^\circ$ (rotations by an average angle of 10° have already been observed;[10] see Fig. 8). For $|\nabla\lambda \cdot \boldsymbol{V}_s| > 1$ the domain rotates (see Fig. 2) with the (average) angular velocity

$$\bar{\omega} = \frac{\sqrt{(\nabla\lambda \cdot \boldsymbol{V}_s)^2 - 1}}{\gamma} \tag{15}$$

and Eq. (13) is solved by

$$\phi(t) = \frac{1}{3}\arctan\left[\frac{1 + \gamma\bar{\omega}\tan(3\bar{\omega}t)}{\sqrt{1+\gamma^2\bar{\omega}^2}}\right], \tag{16}$$

displayed in the inset of Fig. 3. As both γ and $\boldsymbol{V}_s$ are linear in the area A of the domain, $\bar{\omega} \approx (\nabla\lambda \cdot \boldsymbol{V}_s)/\gamma$ becomes independent of the domain size for $A \to \infty$. In this limit, the domain rotates continuously, $\phi = \bar{\omega}t$. Close to the threshold, $\nabla\lambda \cdot \boldsymbol{V}_s = 1$; however, the rotation becomes very slow close to an angle of 15° (plus multiples of 60°).

A way to detect the rotation of the magnetization is to exploit the emergent electric field $\boldsymbol{E}^e$ which obtains a contribution proportional to $\partial_t\phi$ and can be measured in a Hall experiment.[11] In Fig. 3 we therefore show the modulus of the Fourier components, $|c_n| = |\int e^{i6\bar{\omega}nt}\partial_t\phi\, dt|$, of $\partial_t\phi$ as a function of $\nabla\lambda \cdot \boldsymbol{V}_s$. At the threshold, all Fourier components are of equal weight while for large gradients the rotation gets more uniform.

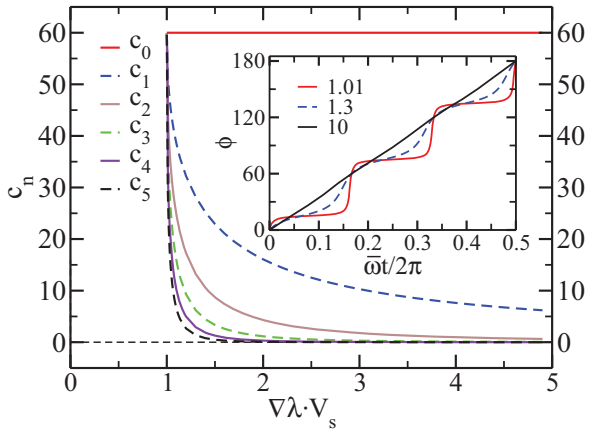

FIG. 3. (Color online) Inset: Rotation angle (in units of 1°) as a function of time for three values of $\nabla\lambda \cdot \boldsymbol{V}_s > 1$; see Eq. (16). For torques close to the value where rotation sets in, the rotation is strongly anharmonic. This can also be seen by considering the Fourier coefficients $c_n = |\int_0^{2\pi/6\bar{\omega}} \partial_t \phi e^{in6\bar{\omega}t}\, dt|$ shown in the main panel as a function of $\nabla\lambda \cdot \boldsymbol{V}_s$.

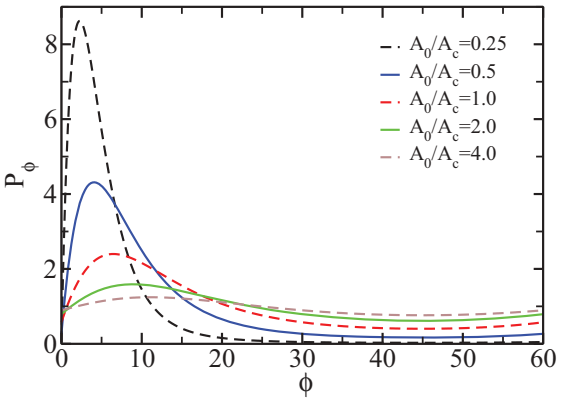

FIG. 4. (Color online) Angular distribution P_ϕ of the rotation angle of the skyrmion lattice for various values of $A_0/A_c \propto \nabla\lambda$ (see text). Here we assumed a distribution of domain sizes of the form $P_d(A) = e^{-A/A_0} A/A_0^2$. While static domains contribute only for $0 \leqslant \phi \leqslant 15^\circ$, one obtains a smooth angular distribution when one takes the rotating domains with $A > A_c$ into account.

For fixed $\bar{\omega}$ the velocities at the boundary of the domain, $v_b = \bar{\omega} r_d$, grow linearly with the radius of the domain r_d. As we have assumed that the gradients across the sample and therefore also across a single domain are small, $r_d\, \nabla\lambda \ll \lambda$, the velocities nevertheless remain small, $v_b \ll |\boldsymbol{V}_s|\lambda/\gamma \lesssim v_s/\tilde{\alpha}$. While our estimate does not rule out that v_b can become somewhat larger than v_s or v_d, we expect that the typical situation is that the velocity v_b arising from the rotation remains smaller than the overall drift velocity of the domain v_d. This estimate also implies that violent phenomena like the breakup of domains due to the rotation will probably not occur.

2. *Domain-size dependence and angular distribution*

In a real system, there will always be a distribution of domain sizes A. Both $\boldsymbol{V}_s$ and γ are linear in A and therefore both the rotation angle Eq. (14) and the angular velocity Eq. (15) will in general depend on the domain size and therefore on the distribution of domains.

Only in the limit $|\nabla\lambda \cdot \boldsymbol{V}_s| \gg 1$ does the dependence on A cancel in Eq. (15) and all domains rotate approximately with the same angular velocity. For $|\nabla\lambda \cdot \boldsymbol{V}_s| \lesssim 1$ one will in general obtain a distribution of rotation angles which can be calculated from the distribution of domain sizes $P_d(A)$. For the static domains only angles up to 15° are possible with

$$P_\phi^s = \int_0^{A_c} dA\, P_d(A) \delta\left(\phi - \frac{\arcsin(A/A_c)}{6}\right) = 6A_c \cos(6\phi)\, P_d[A_c \sin(6\phi)] \quad \text{for } 0 \leqslant \phi \leqslant \frac{\pi}{12}, \quad (17)$$

where $A_c = A/(|\nabla\lambda \cdot \boldsymbol{V}_s|)$ is the size of a "critical" domain which just starts to rotate continuously.

The continuously rotating domains also have a nontrivial angular distribution as their rotation will be slowed down when the counterforces are strongest, i.e., for $\phi = 15^\circ$; see the inset of Fig. 3. The time-averaged angular distribution P_ϕ^r of the rotating domains is calculated from the distribution of domain sizes $P_d(A)$ and the time-averaged angular distribution $p_\phi^r(A)$ of a single domain

$$P_\phi^r = \int_{A_c}^{\infty} dA\, P_d(A)\, p_\phi^r(A),$$
$$p_\phi^r(A) = \frac{1}{T}\int_0^T \delta(\phi - \phi(t))dt = \frac{1}{T\,\partial_t\phi}\Big|_{\phi(t)=\phi} = \frac{3}{\pi}\frac{\sqrt{A^2 - A_c^2}}{A - A_c \sin 6\phi}, \quad (18)$$

where $T = 2\pi/(6\bar{\omega})$. While both P_ϕ^s and P_ϕ^r are nonanalytic at $\phi = 15^\circ$, the total distribution $P_\phi = P_\phi^s + P_\phi^r$ is smooth for $\phi > 0$ and normalized to 1, $\int_0^{2\pi/6} P_\phi\, d\phi = 1$. In Fig. 4 we show P_ϕ, assuming the domain distribution $P_d(A) = e^{-A/A_0}\frac{A}{A_0^2}$ for various values of A_0/A_c.

In elastic neutron scattering, the skyrmion phase is observed by six Bragg spots forming a regular hexagon in a plane perpendicular to the magnetic field. A rotation of the skyrmion domain results in a rotation of these Bragg spots. Therefore the angular distribution P_ϕ of rotation angles is directly observable (see Sec. III D below) by measuring the scattering intensity as a function of angle. By comparing angular distributions for different strengths of the current or gradient, one can—at least in principle—obtain not only A_c as a function of $\nabla\lambda$ or j but also the distribution of domain sizes. The latter can be extracted most easily in the regime where most of the domains do not rotate continuously by plotting $P_\phi/\cos 6\phi$ as a function of $\sin 6\phi$ using Eq. (17).

3. *Dependence on strength of current*

While the behavior of ϕ and $\bar{\omega}$ as a function of $\nabla\lambda$ is rather universal and independent of microscopic details, its dependence on the strength of the current for fixed $\nabla\lambda$ is much more complex. As discussed above, $\boldsymbol{V}_s = \boldsymbol{0}$ for $j < j_c$. Directly at j_c, when the domain starts to move with $v_d \approx 0$,

$\boldsymbol{V}_s$ jumps to the finite value

$$\boldsymbol{V}_s|_{v_s=v_{\rm pin}} = -\frac{A}{4\pi\chi}\left[\left(-\frac{\partial\mathcal{G}\boldsymbol{v}_s}{\partial\lambda}+\frac{\mathcal{G}\boldsymbol{v}_s}{F_{\rm pin}}\frac{\partial F_{\rm pin}}{\partial\lambda}\right) + \hat{\boldsymbol{B}}\times\left(\frac{\partial\mathcal{D}\tilde{\beta}\boldsymbol{v}_s}{\partial\lambda}-\frac{\mathcal{D}\tilde{\beta}\boldsymbol{v}_s}{F_{\rm pin}}\frac{\partial F_{\rm pin}}{\partial\lambda}\right)\right]. \quad (19)$$

Note that the jump is independent of α and α' as well as of their gradients, as the skyrmions are not moving directly at the depinning transition (see Fig. 7). Depending on the direction and size of $\nabla\lambda$, the jump of $\boldsymbol{V}_s$ leads either to a jump of the rotation angle for $|\nabla\lambda\cdot\boldsymbol{V}_s|<1$ or immediately to a continuous rotation for $|\nabla\lambda\cdot\boldsymbol{V}_s|>1$.

Upon increasing the current, $\nabla\lambda\cdot\boldsymbol{V}_s$ can either increase, decrease, or even change its sign depending on (i) the direction of $\nabla\lambda$ and (ii) the question of which of the forces changes most strongly when λ is varied (i.e., temperature or magnetic field).

Motivated by existing experimental data (discussed below in Sec. III D) we study the case of a temperature gradient $\lambda = t$ based on the following assumptions. First, we assume that all damping constants are temperature independent (this assumption is relaxed later). Second, we need also a theory for the temperature dependence of the pinning force. Here we use the experimental observation[11] that the critical current is almost temperature independent at least for a certain range of temperatures. Within our theory, Eqs. (6) and (7), this implies that all temperature dependence of $\boldsymbol{F}_{\rm pin}$ [i.e., the dependence on the parameter t in Eq. (1)] arises from the temperature dependence of the magnetization M which we calculate from the Ginzburg-Landau theory (1). From the Ginzburg-Landau theory, we obtain also the temperature dependence of the other parameters; see Fig. 5.

In Fig. 6 we show a typical result (for temperature-independent dissipation constants) for the rotation angle and angular velocity of a skyrmion domain as a function of $\boldsymbol{v}_s$ in the presence of a temperature gradient. For a temperature gradient perpendicular to the current (lower panel of Fig. 6), the rotation angle increases after the initial jump. For the gradient parallel to the current, however, we obtain that the rotation angle *drops* after the initial jump (upper panel). For larger values of $\boldsymbol{v}_s$ the angle rises again until it reaches its maximal value of 15°. This qualitative shape of the curve appears to be rather independent

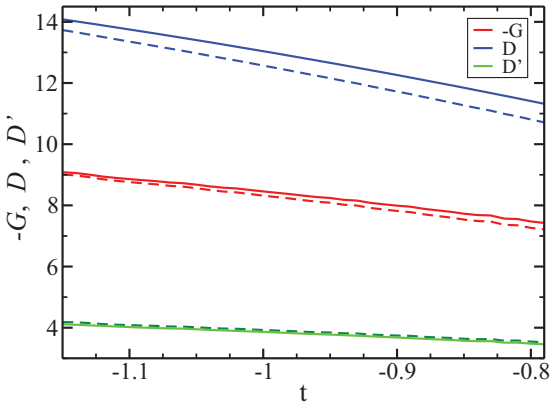

FIG. 5. (Color online) Change of $\mathcal{G},\mathcal{D}$, and $\mathcal{D}'$ defined in Eq. (6) with temperature t. The applied magnetic field is $h/\sqrt{2}(0,0,1)$. Dashed lines are for $h=0.9$ and continuous lines for $h=1.1$.

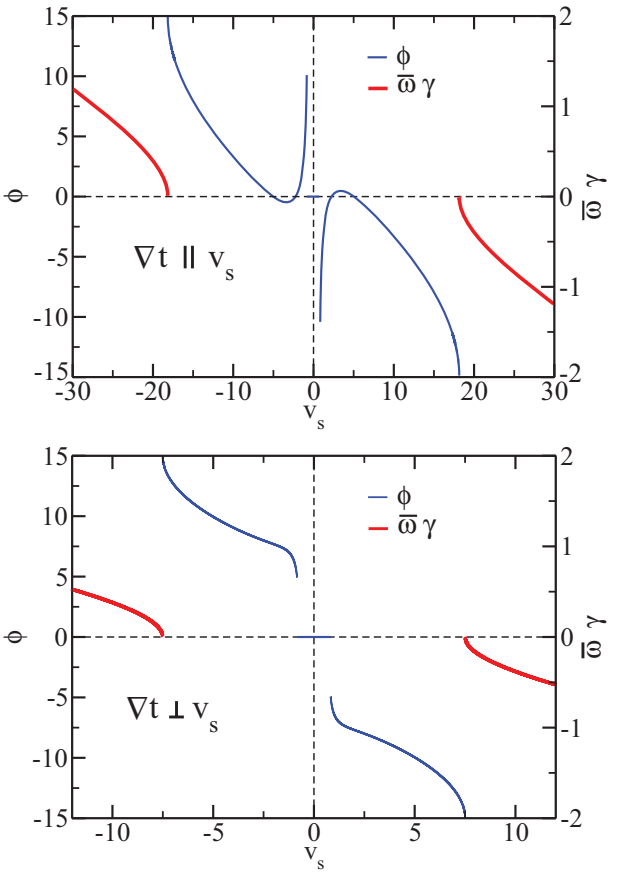

FIG. 6. (Color online) Rotation angle ϕ (in units of 1°) and angular velocity $\gamma\bar{\omega}$ as functions of v_s for a temperature gradient parallel [$\nabla t \parallel \boldsymbol{v}_s$, $\nabla t=(-0.1,0,0)$, upper panel] and perpendicular [$\nabla t \perp \boldsymbol{v}_s$, $\nabla t=(0,-0.05,0)$, lower panel] to the current [$\alpha=0.2,\beta=0.45,\alpha'=0.01,\beta'=0.2,A/\chi=200,t=-1,\boldsymbol{B}=(0,0,1/\sqrt{2}),v_{\rm pin}=1,f=1$]. For both geometries one observes a jump of ϕ at $v_s\approx v_{\rm pin}$ from zero to a finite rotation angle. After the initial jump the rotation angle increases for the perpendicular configuration (b) while for the parallel arrangement first a drop and then an increase up to the maximal angle of 15° occurs. For larger v_s a continuous rotation characterized by the angular velocity $\bar{\omega}$ sets in for both configurations. For the calculation we assumed that the damping parameters and $v_{\rm pin}$ are independent of t.

of the precise values of the various parameters *if* we assume that all damping parameters are temperature independent.

In Fig. 7 we plot the rotation angle for small current densities, taking an extra effect into account which is present in the experiments described in Ref. 10: as the temperature gradients are induced by the currents, they grow quadratically with v_s. This does not give rise to any qualitative changes. The thin blue curve in Fig. 7 thereby reflects the same physics as the corresponding curve in Fig. 6 (note the different scale on the x axis). The thick green curve of Fig. 7 shows that one can, however, obtain qualitatively different results (an increase rather than a reduction of the rotation angle after the initial jump for T gradients parallel to the current, upper panel) by including a small temperature dependence of the Gilbert damping α. As we will discuss in Sec. III D, this can reproduce qualitatively the experimentally observed behavior.

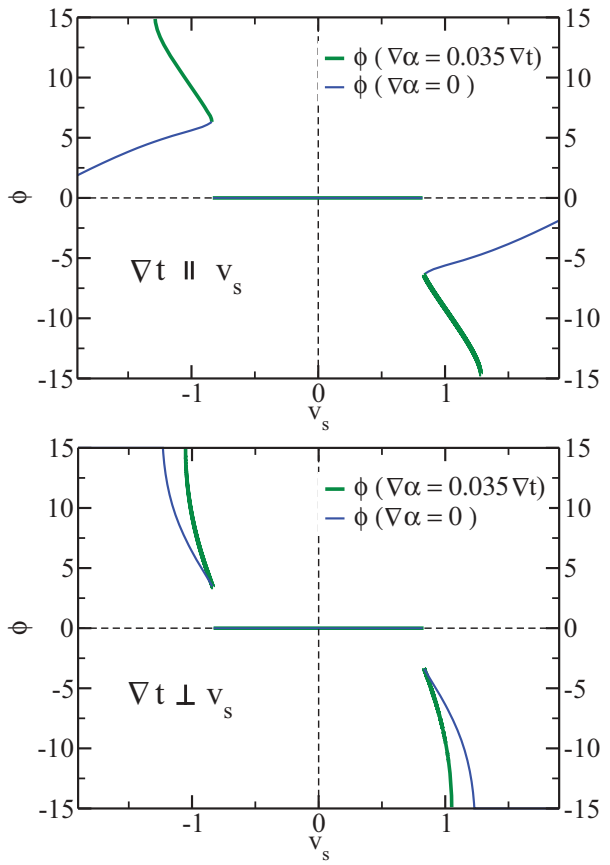

FIG. 7. (Color online) Rotation angle ϕ (in units of 1°) as a function of v_s for a temperature gradient parallel ($\nabla t \parallel \boldsymbol{v}_s$, upper panel) and perpendicular ($\nabla t \perp \boldsymbol{v}_s$, lower panel) to the current. The parameters are the same as in Fig. 6 with two exceptions. First, we have taken into account that in the experiments of Ref. 10 the temperature gradient grows with the square of the applied current, $\nabla t = (-0.1v_s^2,0,0)$ and $\nabla t = (0,-0.05v_s^2,0)$, for current parallel and perpendicular to $\boldsymbol{v}_s$, respectively. For the thin blue curve we assumed (as in Fig. 6) that the damping constants are independent of t while for the thick green curve a weak temperature dependence of the damping constant α, $\nabla\alpha = 0.035\nabla t$, was assumed. This parameter has been chosen to reflect the experimental observation; see Fig. 8. For even stronger currents (not measured experimentally and not shown in the figure) the size of the torque drops again and a finite rotation angle is obtained for $1.57 \lesssim v_s \lesssim 2.53$ in the parallel configuration with the temperature-dependent damping constant.

4. Dependence on orientation of gradients

Figure 6 shows that the rotational torques on the system depend strongly on the relative orientation of gradient and current. More importantly, one probes different physical mechanism for gradients parallel or perpendicular to the current. This effect was already discussed in the Introduction (see Fig. 1), where, however, only the simple case of a static domain without pinning was described. In reality, the situation is more complex. All directional information is encoded in the function $\boldsymbol{V}_s[\boldsymbol{v}_s]$ which can be obtained by first solving Eq. (6) to obtain $\boldsymbol{v}_d$ and then comparing Eqs. (12) and (13). Unfortunately, a rather large number of unknown parameters (most importantly, the pinning forces and their dependence on λ) enters the description. Therefore we will discuss in the following only a few limiting cases.

A drastically simplified picture occurs in regimes when only two forces dominate in Eq. (6). For example, close to the depinning transition, the Magnus force is of the same order as the pinning force while the two dissipative forces are typically much smaller. In this case one can use Eq. (6) to show that $\hat{\boldsymbol{v}}_d$ becomes proportional to $\hat{\boldsymbol{B}} \times (\boldsymbol{v}_s - \boldsymbol{v}_d)$. Thus, for an λ-independent $\boldsymbol{v}_s$, both the reactive rotational coupling vector and the rotational pinning vector become proportional to $\nabla\lambda \cdot (\boldsymbol{v}_s - \boldsymbol{v}_d)$. Therefore the *ratio* of the components of $\boldsymbol{V}_s$ parallel ($\boldsymbol{V}_s{}^{\parallel}$) and perpendicular ($\boldsymbol{V}_s{}^{\perp}$) to $\boldsymbol{v}_s$ depends only on the direction in which the skyrmion lattice drifts:

$$\frac{\boldsymbol{V}_s{}^{\parallel}}{\boldsymbol{V}_s{}^{\perp}} \approx \frac{(\boldsymbol{v}_s - \boldsymbol{v}_d)^{\parallel}}{(\boldsymbol{v}_s - \boldsymbol{v}_d)^{\perp}} = -\frac{v_d^{\perp}}{v_d^{\parallel}}. \tag{20}$$

The ratio $\frac{\boldsymbol{V}_s{}^{\parallel}}{\boldsymbol{V}_s{}^{\perp}}$ can be obtained experimentally by measuring the rotation angle or the angular velocity for $\nabla\lambda$ parallel and perpendicular to the current, from which one can obtain directly $\frac{\boldsymbol{V}_s{}^{\parallel}}{\boldsymbol{V}_s{}^{\perp}}$ using Eqs. (14) and (15). For small angles, $\arcsin x \approx x$, for example, one obtains $\frac{\boldsymbol{V}_s{}^{\parallel}}{\boldsymbol{V}_s{}^{\perp}}$ directly from the ratio of the two rotation angles. A different, but probably more precise, way to determine this ratio is to find experimentally the "magic angle" ϕ_m of gradient vs current, where all rotations vanish, $\nabla\lambda \cdot \boldsymbol{V}_s = 0$. In this case one obtains

$$\frac{\boldsymbol{V}_s{}^{\parallel}}{\boldsymbol{V}_s{}^{\perp}} = \frac{1}{\tan\phi_m}. \tag{21}$$

This should allow for a quantitative determination of $v_d^{\perp} / v_d^{\parallel}$. As $v_d^{\parallel}$ can be measured independently using emergent electric fields generated by the motion of skyrmions,[11] one can obtain the complete information on the drift motion by combining both experiments. It is also instructive to compare skyrmions and vortices in a superconductor. Vortices and skyrmions follow essentially the same equation of motion, Eq. (6). The relevant parameters (and therefore also the pinning physics) are, however, rather different. For vortices in conventional superconductors[20,33] the dissipation is very large, $\mathcal{D}\alpha \gg \mathcal{G}$. Therefore, vortices drift—up to small corrections—predominantly *perpendicular* to the current while for magnetic skyrmions we expect that, at least not too close to the depinning transition, the motion is dominantly parallel to the current.

In the limit where the pinning forces can be neglected, i.e., $v_s \gg v_{\text{pin}}$, to linear order in $\tilde{\beta}$ and $\tilde{\alpha}$ the vector $\boldsymbol{V}_s$ is given by

$$\boldsymbol{V}_s = -\frac{A}{4\pi\chi}(\hat{\boldsymbol{B}} \times \boldsymbol{v}_s)\left((\tilde{\beta} - \tilde{\alpha})\frac{\partial\mathcal{G}}{\partial\lambda}\frac{\mathcal{D}}{\mathcal{G}} + \frac{\partial\mathcal{D}(\tilde{\beta} - \tilde{\alpha})}{\partial\lambda}\right) \tag{22}$$

$$= -\frac{A}{4\pi\chi}\left(\hat{\boldsymbol{B}} \times \boldsymbol{v}_s\right)\frac{1}{\mathcal{G}}\frac{\partial}{\partial\lambda}(\mathcal{D}\mathcal{G}(\tilde{\beta} - \tilde{\alpha})). \tag{23}$$

Here we also neglected a possible λ dependence of v_s. In this limit the rotation can be induced primarily by gradients perpendicular to $\boldsymbol{v}_s$, reflecting that the motion of skyrmions is mainly parallel to the current; see Eqs. (8) and (20). This is also consistent with the behavior shown in Fig. 6 where we used a two-times smaller gradient for the perpendicular configuration and obtained nevertheless an onset of the rotational motion for

values of v_s much smaller than in the parallel configuration. Note that in a Galilean-invariant system, $\tilde{\alpha} = \tilde{\beta}$, no torques can be expected.

D. Experimental situation

Our study is directly motivated by recent neutron scattering experiments in the skyrmion lattice phase of MnSi.[10] In the presence of a sufficiently large current, a rotation of the magnetic diffraction pattern by a finite angle was observed when simultaneously a temperature gradient was present (only temperature gradients parallel to the current have been studied). The rotation angle could be reversed by reversing either the direction of the current, the direction of the magnetic field, or the direction of the temperature gradient. This clearly showed that rotational torques in the experiment were driven by the interplay of gradients and currents as studied in this paper.

In Fig. 8(a) we reproduce Fig. 3(A) of Ref. 10, which shows the average rotation angle (defined as the maximum of the azimuthal distribution of the scattering intensity) as a function of current density. Above a critical current, $j > j_c$, the rotation sets in. The rotation angle initially increases abruptly, followed by a slower increase for larger current densities. When comparing these results with our theory one has to take into account that the temperature gradient in the experiment was not independent of the strength of the applied electrical current density as it originated in the resistive heating in the sample. Therefore the temperature gradient was growing with j^2 (i.e., the heating rate due to the electric current). This was taken into account in Fig. 7 as discussed above. For a full quantitative comparison of theory and experiment, it would be desirable to have data where the applied current as well as both the strength and the direction of the gradients are changed independently. As such data are presently not available, we restrict ourselves to a few more qualitative observations.

In our theory we expect a jump of the rotation angle at j_c, which depends on the domain size. This appears to be consistent with the steep increase of the rotation angle as observed experimentally at j_c, especially when taking into account that the experimental results are subject to a distribution of domain sizes.

Interestingly, the experimentally observed increase of the rotation angle after its initial jump is apparently *not* consistent with the predictions from the extended Landau-Lifshitz-Gilbert equation shown in Eq. (2) *if* we assume that $\alpha,\alpha',\beta,\beta'$ are independent of temperature. As shown in Fig. 7, we can, however, describe the experimentally observed behavior if we assume a weak temperature dependence of the Gilbert damping.

An important question concerns whether the existing experiments already include evidence of some larger domains that rotate continuously. Figure 8(a) shows that for the largest currents *average* rotation angles of up to 10° have been obtained. As this is rather close to the maximally possible value of 15° for static domains, it suggests that continuously rotating domains either are already present in the system or may be reached by using slightly larger currents or temperature gradients.

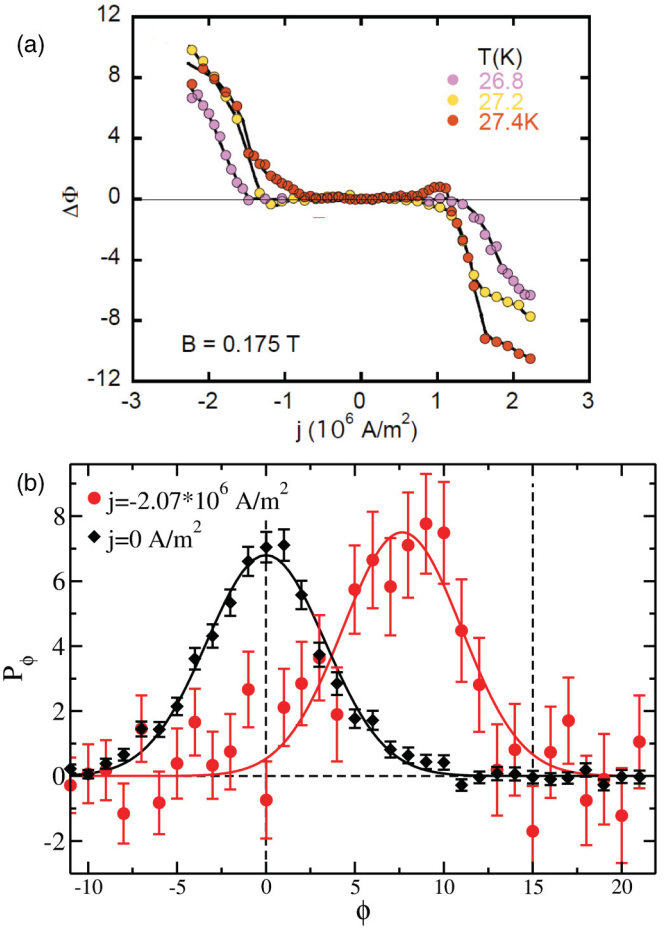

FIG. 8. (Color online) (a) Average rotation angle $\Delta\phi$ (in units of 1°) of the skyrmion lattice in MnSi measured by neutron scattering in the presence of an electric current and a temperature gradient parallel to the current. The figure is taken from Ref. 10, where further details on the experimental setup can be found. (b) Angular distribution P_ϕ of the intensity normalized to 1 for currents of strength $j = 0$ (black diamonds) and $j \approx -2.07 \times 10^6$ A/m^2 for $T = 27.4$ K (red circles). The lines are Gaussian fits serving as a guide to the eye. The distribution of angles extends up to the maximally possible rotation angle of 15°, which suggests that some of the larger domains are rotating with finite angular velocity for this parameter range.

We have therefore investigated the angular distribution of the scattering pattern using the same set of experimental data analyzed in Ref. 10 (technical details of the experimental setup are reported in this paper). In Fig. 8(b) we show the azimuthal intensity distribution with and without applied current. Already for zero current a substantial broadening of the intensity distribution is observed. The origin of this broadening lies in demagnetization effects which lead to small variations of the orientation of the local magnetic fields in the sample, tracked closely by the skyrmions. It has been shown[14] that this effect can be avoided in thin samples when only the central part of this sample is illuminated. For the existing data this implies that a quantitative analysis of P_ϕ is not possible. We observed that the measured experimental distribution of angles extends up just to 15°. Therefore, from the present data we can neither claim nor exclude that continuously rotating domains already exist for this set of data but slightly larger

current densities or gradients should be sufficient to create those.

IV. CONCLUSIONS

The magnetic skyrmion lattices first observed in MnSi have by now been observed in a wide range of cubic, chiral materials including insulators,[36,37] doped semiconductors,[38] and good metals.[9,39] This is expected from theory: in any material with $B20$ symmetry, which would be ferromagnetic in the absence of spin-orbit coupling, weak Dzyaloshinskii-Moriya interactions induce skyrmion lattices in a small magnetic field. While in bulk they are stabilized only in a small temperature window by thermal fluctuations close to the critical temperature, they are much more stable in thin films.[12,13]

From the viewpoint of spintronics, such skyrmions are ideal model systems to investigate the coupling of electric, thermal, or spin currents to magnetic textures: (i) the coupling by Berry phases to the quantized winding number provides a universal mechanism to create Magnus forces efficiently, (ii) the skyrmion lattice can be manipulated by extremely small forces induced by ultrasmall currents,[10,11] and (iii) the small currents imply that new types of experiments (e.g., neutron scattering on bulk samples) are also possible.

We think that the investigation of the rotational dynamics of skyrmion domains provides a very useful method to study in more detail which forces affect the dynamics of the magnetic texture. As we have shown, the rotational torques can be controlled by both the strength and the direction of field or temperature gradients in combination with electric currents. They react very sensitively not only to the relative strength of the various forces but also to how the forces depend on temperature and field.

While some aspects of the theory, e.g., the dependence on the strength of the gradients, can be worked out in detail, many other questions remain open. An important concern is, for example, to identify the leading damping mechanisms and their dependence on temperature and field. Also, an understanding of the interplay of pinning physics, damping, and the motion of magnetic textures is required to control spin-torque effects. Here future rotation experiments are expected to give valuable information. Furthermore, it will be interesting to study the pinning physics in detail and to learn to what extent skyrmions and vortices in superconductors behave differently.

One way to observe the rotation of the skyrmion lattice is to investigate the angular distribution of the neutron scattering pattern as discussed in Sec. III C. This, however, provides only indirect evidence for the expected continuous rotation of the skyrmion lattice. Therefore it would be interesting to observe the continuous rotation more directly. For example, one can use the fact that time-dependent Berry phases arising from moving skyrmions induce emergent electrical fields which can be directly measured[11] in a Hall experiment. Here it would be interesting to observe higher harmonics in the signal, which are expected to appear close to the threshold where continuous rotations set in; see Fig. 3.

In future, it might also be interesting to use instead of electrical current other methods, e.g., pure spin currents or thermal currents, to manipulate skyrmion lattices (e.g., in insulators). We expect that in such systems also the investigation of rotational motion driven by gradients will give useful insight into the control of magnetism beyond thermal equilibrium.

ACKNOWLEDGMENTS

We gratefully acknowledge discussions with M. Halder, M. Mochizuki, and T. Nattermann. We also acknowledge financial support of the German Science Foundation (DFG) through SFB 608, TRR80, and FOR960, as well as the European Research Council through ERC-AdG (Grant No. 291079). K.E. wishes to thank the Deutsche Telekom Stiftung and the Bonn Cologne Graduate School.

[1] M. Tsoi, A. G. M. Jansen, J. Bass, W.-C. Chiang, M. Seck, V. Tsoi, and P. Wyder, Phys. Rev. Lett. **80**, 4281 (1998).
[2] E. Myers, D. Ralph, J. Katine, R. Louie, and R. Buhrman, Science **285**, 867 (1999).
[3] S. Kiselev, J. Sankey, I. Krivorotov, N. Emley, R. Schoelkopf, R. Buhrman, and D. Ralph, Nature (London) **425**, 380 (2003).
[4] J. Grollier, P. Boulenc, V. Cros, A. Hamzi, A. Vaurs, A. Fert, and G. Faini, Appl. Phys. Lett. **83**, 509 (2003).
[5] M. Tsoi, R. Fontana, and S. Parkin, Appl. Phys. Lett. **83**, 2617 (2003).
[6] S. S. P. Parkin, M. Hayashi, and L. Thomas, Science **320**, 190 (2008).
[7] J. Slonczewski, J. Magn. Magn. Mater. **159**, L1 (1996).
[8] L. Berger, Phys. Rev. B **54**, 9353 (1996).
[9] S. Mühlbauer, B. Binz, F. Jonietz, C. Pfleiderer, A. Rosch, A. Neubauer, R. Georgii, and P. Böni, Science **323**, 915 (2009).
[10] F. Jonietz, S. Mühlbauer, C. Pfleiderer, A. Neubauer, W. Münzer, A. Bauer, T. Adams, R. Georgii, P. Böni, R. A. Duine *et al.*, Science **330**, 1648 (2010).
[11] T. Schulz, R. Ritz, A. Bauer, M. Halder, M. Wagner, C. Franz, C. Pfleiderer, K. Everschor, M. Garst, and A. Rosch, Nat. Phys. **8**, 301 (2012).
[12] X. Z. Yu, Y. Onose, N. Kanazawa, J. H. Park, J. H. Han, Y. Matsui, N. Nagaosa, and Y. Tokura, Nature (London) **465**, 901 (2010).
[13] X. Z. Yu, Y. Onose, N. Kanazawa, J. H. Park, J. H. Han, Y. Matsui, N. Nagaosa, and Y. Tokura, Nat. Mater. **10**, 106 (2011).
[14] T. Adams, S. Mühlbauer, C. Pfleiderer, F. Jonietz, A. Bauer, A. Neubauer, R. Georgii, P. Böni, U. Keiderling, K. Everschor *et al.*, Phys. Rev. Lett. **107**, 217206 (2011).
[15] V. S. Pribiag, I. N. Krivorotov, G. D. Fuchs, P. M. Braganca, O. Ozatay, J. C. Sankey, D. C. Ralph, and R. A. Buhrman, Nat. Phys. **3**, 498 (2007).
[16] A. V. Khvalkovskiy, J. Grollier, A. Dussaux, K. A. Zvezdin, and V. Cros, Phys. Rev. B **80**, 140401 (2009).
[17] A. Schmid and W. Hauger, J. Low Temp. Phys. **11**, 667 (1973).
[18] A. I. Larkin and Y. N. Ovchinnikov, Sov. Phys. JETP **38**, 854 (1974).
[19] T. Nattermann, S. Stepanow, L.-H. Tang, and H. Leschhorn, J. Phys. II **2**, 1483 (1992).

[20]G. Blatter, M. V. Feigel'man, V. B. Geshkenbein, A. I. Larkin, and V. M. Vinokur, Rev. Mod. Phys. **66** (1994).
[21]K. Everschor, M. Garst, R. A. Duine, and A. Rosch, Phys. Rev. B **84**, 064401 (2011).
[22]A. A. Thiele, Phys. Rev. Lett. **30**, 230 (1972).
[23]Y. Tserkovnyak and C. H. Wong, Phys. Rev. B **79**, 014402 (2009).
[24]S. Zhang and S. S.-L. Zhang, Phys. Rev. Lett. **102**, 086601 (2009).
[25]J. Zang, M. Mostovoy, J. H. Han, and N. Nagaosa, Phys. Rev. Lett. **107**, 136804 (2011).
[26]O. Nakanishi, A. Yanase, A. Hasegawa, and M. Kataoka, Solid State Commun. **35**, 995 (1980).
[27]P. Bǻk and M. H. Jensen, J. Phys. C **13**, L881 (1980).
[28]G. Tatara and H. Kohno, Phys. Rev. Lett. **92**, 086601 (2004).
[29]S. Zhang and Z. Li, Phys. Rev. Lett. **93**, 127204 (2004).
[30]The spin current j_s^{ji} is a tensor describing the current of the spin component j flowing in the direction i. To describe spin torques, the projection of j_s^{ji} on the local direction of the magnetization is needed, $j_s^i = \hat{\boldsymbol{\Omega}}_j j_s^{ji}$ and $\boldsymbol{v}_s \approx \boldsymbol{j}_s/|\boldsymbol{M}|$.
[31]G. Volovik, J. Phys. C **20**, L83 (1987).
[32]In a previous publication (Ref. 21) we have defined $\boldsymbol{G}$ and $\boldsymbol{D}$ without the factors M which need to be included here for the discussion of gradients.
[33]N. Kopnin, Rep. Prog. Phys. **65**, 1633 (2002).
[34]O. A. Tretiakov, D. Clarke, G.-W. Chern, Y. B. Bazaliy, and O. Tchernyshyov, Phys. Rev. Lett. **100**, 127204 (2008).
[35]D. J. Clarke, O. A. Tretiakov, G.-W. Chern, Y. B. Bazaliy, and O. Tchernyshyov, Phys. Rev. B **78**, 134412 (2008).
[36]S. Seki, X. Z. Yu, S. Ishiwata, and Y. Tokura, Science **336**, 198 (2012).
[37]T. Adams, A. Chacon, M. Wagner, A. Bauer, G. Brandl, B. Pedersen, H. Berger, P. Lemmens, and C. Pfleiderer, Phys. Rev. Lett. **108**, 237204 (2012).
[38]W. Münzer, A. Neubauer, T. Adams, S. Mühlbauer, C. Franz, F. Jonietz, R. Georgii, P. Böni, B. Pedersen, M. Schmidt *et al.*, Phys. Rev. B **81**, 041203(R) (2010).
[39]C. Pfleiderer, T. Adams, A. Bauer, W. Biberacher, B. Binz, F. Birkelbach, P. Böni, C. Franz, R. Georgii, M. Janoschek *et al.*, J. Phys.: Condens. Matter **22**, 164207 (2010).